Journal for ImmunoTherapy of Cancer

Stromal LAG-3$^+$ cells infiltration defines poor prognosis subtype muscle-invasive bladder cancer with immunoevasive contexture

Han Zeng,[1] Quan Zhou,[1] Zewei Wang,[2] Hongyu Zhang,[1] Zhaopei Liu,[1] Qiuren Huang,[1] Jiajun Wang,[2] Yuan Chang,[3] Qi Bai,[2] Yu Xia,[2] Yiwei Wang,[4] Le Xu,[5] Bo Dai,[3] Jianming Guo,[2] Li Liu,[2] Yu Zhu,[3] Jiejie Xu [1]

To cite: Zeng H, Zhou Q, Wang Z, *et al*. Stromal LAG-3$^+$ cells infiltration defines poor prognosis subtype muscle-invasive bladder cancer with immunoevasive contexture. *Journal for ImmunoTherapy of Cancer* 2020;**8**:e000651. doi:10.1136/jitc-2020-000651

► Additional material is published online only. To view, please visit the journal online (http://dx.doi.org/10.1136/jitc-2020-000651).

HZ, QZ, ZW and HZ contributed equally.

Accepted 07 May 2020

For numbered affiliations see end of article.

Correspondence to
Prof Jiejie Xu;
jjxufdu@fudan.edu.cn

Dr Yu Zhu;
yuzhu10@fudan.edu.cn

Dr Li Liu;
liu.li@zs-hospital.sh.cn

ABSTRACT

Background Lymphocyte activation gene 3 (LAG-3) is a promising immune checkpoint therapeutic target being evaluated in clinical trials. We assessed the LAG-3$^+$ cells distribution, its association with clinical outcomes and immune contexture and its role in the landscape of muscle-invasive bladder cancer (MIBC) treatment.

Methods 141 patients with MIBC from Zhongshan Hospital were included for survival and adjuvant chemotherapy (ACT) benefit analyses. 32 fresh resected samples of MIBC were collected to detect CD8$^+$ T cells functional state. The molecular classification analyses were based on 391 patients with MIBC from The Cancer Genome Atlas. Immunohistochemistry and flow cytometry were performed to characterize various immune cells infiltration.

Results In Kaplan-Meier analyses and Cox regression models, stromal LAG-3$^+$ cells enrichment was consistently associated with inferior overall survival and disease-free survival, and indicated suboptimal responsiveness to ACT. Patents with high stromal LAG-3$^+$ cells possessed increased protumor cells, immunosuppressive cytokines and immune checkpoint expression. The phenotypic analyses of CD8$^+$ T cells correlated its dysfunctional state with LAG-3$^+$ cells. Besides, LAG-3 mRNA level was linked to luminal and basal subtypes of MIBC. LAG-3-high tumors exhibited limited FGFR3 mutation and signaling signature, and displayed activated immunotherapeutic and EGFR-associated pathway.

Conclusions Stromal LAG-3$^+$ cells abundance indicated an immunoevasive contexture with dysfunctional CD8$^+$ T cells, and represented an independent predictor for adverse survival outcome and ACT resistance in MIBC. LAG-3 expression could potentially be a novel biomarker for FGFR3-targeted and EGFR-targeted therapies and immunotherapy. The crucial role of LAG-3$^+$ cells in the therapeutic landscape of MIBC needs further validation retrospectively and prospectively.

INTRODUCTION

Muscle-invasive bladder cancer (MIBC) is an advanced disease with aggressive properties and high mortality.[1] Clinical guidelines have established radical cystectomy (RC) as the mainstay of treatment for MIBC, and recommended cisplatin-based neoadjuvant chemotherapy (NACT) for eligible patients to improve prognosis.[2] Theoretically, the efficacy of adjuvant chemotherapy (ACT) should be comparable with NACT, but substantial adverse reaction, chemotherapeutic resistance and deteriorated condition of patients with MIBC limited the implementation of ACT practically.[3 4] Considering guidelines' acceptance of cisplatin-based ACT under conditions of NACT absence and the low ratio of worldwide NACT application in MIBC,[2] further analyses for identifying responders to ACT is clinically needed to guide the individualized approach to chemotherapy.

Recently, advances in characterization of molecular-profiling and immune-profiling show potential to remodel the paradigm of MIBC treatment. Molecular-profiling of MIBC has screened several novel therapeutic targets, including fibroblast growth factor 3 (FGFR3, BLC2001 trial) and epidermal growth factor receptor (EGFR, BL-2007–02 trial), which are overexpressed in tumors and confer poor survival outcome.[5 6] Besides, reported as an immunogenic malignancy, MIBC can response durably to immune checkpoint blockade (ICB).[7] Continuing clinical trials are evaluating prospects of ICB targeting programmed cell death-1 (PD-1)-programmed death-ligand 1 (PD-L1) axis and cytotoxic T-lymphocyte-associated protein 4 (CTLA-4) as first-line treatment for advanced bladder cancer. Although assessment of immuno-oncology and immune microenvironment are developing in full swing, researches concentrating on investigating immune checkpoints (ICKs) expression in MIBC remain scarce. Lymphocyte activation gene 3 (LAG-3) is identified as a possible

target of ICB, and its clinical significance in MIBC is unexplored.

As a transmembrane protein discovered in 1990, LAG-3 is expressed on activated T cells and natural killer cells.[8 9] Many preclinic studies have confirmed that LAG-3 signaling led to cytotoxic $CD8^+$ T cells exhaustion, and LAG-3 blockade can synergize with PD-1/PD-L1 therapy to reinvigorate antitumor immunity.[10] However, the prognostic value of LAG-3^+ cells remains inconsistent in different types of cancer. In breast cancer and ovarian cancer, LAG-3^+ cells abundance indicated improved prognosis and might be the counterbalance reaction to the ongoing antitumor T-cell immunity.[11 12] Inversely, LAG-3^+ cells infiltration was associated with poor survival in non-small cell lung cancer,[13] representing an immunosuppressive landscape. Herein, our purpose was to elucidate the prognostic significance of LAG-3^+ cells and its relationship with ACT benefit and immune contexture in MIBC. Meanwhile, the association of LAG-3 mRNA expression with molecular subtypes and targeted therapy was studied based on The Cancer Genome Atlas (TCGA). Our results first illustrated that the multiple clinical value of LAG-3^+ cells could possibly usher personalized treatment for MIBC.

MATERIALS AND METHODS

Study population and mRNA data

This study enrolled 215 patients treated with RC from Zhongshan Hospital cohort (ZSHC, surgery date: 2002–2014) of Fudan University. Formalin-fixed paraffin-embedded samples of ZSHC were sectioned by tissue microarray (TMA) technology. Seventy-four patients were excluded according to the following criteria: 1) informed consent; 2) accessible for complete clinical and prognostic data; 3) diagnosed as MIBC (73 excluded: 13 non-urothelial carcinoma, 60 pathological Ta/Tis/T1); 4) without other therapies besides cisplatin-based ACT and RC; 5) no detachment in TMA (1 excluded). Follow-up information was collected routinely according to guidelines until July 2016.[2] The clinical-pathological characteristics of 141 patients with MIBC are presented in table 1.

The mRNA sequencing data of bladder cancer (BLCA) in TCGA was downloaded from http://www.cbioportal.org/ in May 2018. The molecular subtype information of patients was derived using R package *BLCAsubtyping* (https://github.com/cit-bioinfo/BLCAsubtyping). Twenty-one patients were excluded for consistence: 7 patients without survival data or sequencing data, 4 patients with pathological non-MIBC and 10 patients with NACT application. The RNA-seq data were obtained as Fragments Per Kilobase of transcript per Million mapped reads (FPKM), and the mRNA expression of 391 patients with MIBC from TCGA were normalized by the formula $\log_2$(FPKM+1) before analyses. The involved signatures were defined from previous studies and scored as the average of related genes expression (online supplementary table 1).

Assay methods

Single and double immunohistochemical (IHC) staining were carried out according to the protocols as detailed previously.[14 15] Digitally scanned with NanoZoomer-XR (Hamamatsu) and image Pro Plus 6.0, TMA sections were independently reviewed by two pathologists who were blinded to clinical information. The density of LAG-3^+ cells and other immune cells were evaluated as the mean of cells infiltration in six representative fields (each pathologist with three fields). The specific information and representative images of identified immune cells are illustrated in online supplementary table 2 and online supplementary figure 1, respectively. As the distribution of LAG-3^+ cells in the tumor bed showed significant difference, pathologists separately counted intraepithelial and stromal LAG-3^+ cells number under high-power (400×) magnification filed (HPF). Stromal LAG-3^+ cells (sLAG-3^+ cells) were evaluated as positive cells not directly interacted with the tumor nests, whereas intraepithelial LAG-3^+ cells (iLAG-3^+ cells) were counterparts located within the tumor nests with no intervening stroma. Total tumor-infiltrating LAG-3^+ cells count was defined as the sum of stromal and intraepithelial compartments. The intraclass correlation between the two pathologists' evaluations for tumor-infiltrating LAG-3^+ cells, iLAG-3^+ cells and sLAG-3^+ cells from the same slide were 0.931 (95% CI: 0.895 to 0.952, p<0.001), 0.858 (95% CI: 0.793 to 0.905, p<0.001) and 0.938 (95% CI: 0.903 to 0.961, p<0.001), respectively. Any positive infiltration (≥1 cells/HPF) was applied to define positive and negative iLAG-3^+ cells infiltration, and commonly used median value (tumor-infiltrating LAG-3^+ cells: 11.67 cells/HPF; sLAG-3^+ cells: 10 cells/HPF) was applied to dichotomize population as low and high subgroup.

Fresh resected tumor tissues of 32 patients with MIBC were obtained from Zhongshan Hospital, Fudan University Shanghai Cancer Center, Ruijin Hospital and Shanghai General Hospital. Collected surgical tumor tissues were digested into single-cell suspension with collagenase V (Sigma), and then incubated with RBC lysis buffer (BD). After FVS510 (BD) was applied to identify alive cells, cell suspensions were incubated with Fc block (BD). Next, isolated cells were stained with membrane markers (CD45-ApcCy7-conjugated, CD8-BB515-conjugated, PD-1-AF647-conjugated, T-cell immunoglobulin mucin-3 [TIM-3]-PE-conjugated (BD); LAG-3-BV785-conjugated, CTLA-4-BV605-conjugated (Biolegend) and T cell immunoreceptor with Ig and ITIM domains [TIGIT]-AF700-conjugated (R&D) antibodies) for 40 min at 4°C. After cells were fixed by Fixation/Permeabilization Kit (BD) or Transcription Factor Buffer Set (BD) according to manufacturer's protocol, IFN-γ-PeCy7-conjugated, Granzyme B (GZMB)-AF647-conjugated, PRF-1-PE-conjugated (BD) and Ki-67-AF700-conjugated (Biolegend) antibodies were used for further staining. Stained cells were resuspended in cell staining buffer, tested on BD FACSCelesta and then analyzed via FlowJo V.10.0.7 (Tree Star). After cells were gated according to negative control (Fluorescence Minus

Table 1 Association of iLAG-3$^+$ cells and sLAG-3$^+$ cells with clinicopathological parameters

	Patients		sLAG-3$^+$ cells infiltration			iLAG-3$^+$ cells infiltration		
			Low (n=70)	High (n=71)		Negative (n=73)	Positive (n=68)	
Parameters	No.	%	(<10 cells/HPF)	(≥10 cells/HPF)	P value*	(<1 cells/HPF)	(≥1 cells/HPF)	P value*
Age at surgery (year)					0.195†			0.678†
Median (IQR)	62.0 (56–71)		61.5 (54–72)	64.0 (58–71)		62.0 (56–72)	62.5 (56–69)	
Gender					0.191			0.248
Male	117	83	61	56		58	59	
Female	24	17	9	15		15	9	
Tumor size (cm)					0.291†			0.431†
Median (IQR)	3.5 (2.5–5.0)		4.0 (2.3–6.0)	3.5 (2.5–4.0)		3.0 (2.5–5.0)	4.0 (2.5–5.0)	
AJCC stage					**0.002**			0.679
II	87	61.7	53	34		45	42	
III	46	32.6	16	30		25	21	
IV	8	5.7	1	7		3	5	
pT stage					**0.014**			0.170
pT2	90	63.8	53	37		47	43	
pT3	30	21.3	10	20		12	18	
pT4	21	14.9	7	14		14	7	
pN stage					0.063			0.482
pN0	133	94.3	69	64		70	63	
pN+	8	5.7	1	7		3	5	
Grade					0.067			0.480
Low	24	17	16	8		14	10	
High	117	83	54	63		59	58	
LVI					0.070			0.978
Absent	52	36.9	31	21		27	25	
Present	89	63.1	39	50		46	43	
ACT					0.447			0.359
Applied	69	48.9	32	37		33	36	
Not applied	72	51.1	38	34		40	32	

Tumor stage was updated according to AJCC 2017 classification.
*P value from Fisher's exact test was used when data fail to meet the requirement of χ^2 test; significant p value < 0.05 was shown in bold.
†Mann-Whitney U test.
ACT, adjuvant chemotherapy; AJCC, American Joint Committee on Cancer; HPF, high-power field; iLAG-3$^+$, intraepithelial LAG-3$^+$; LVI, lymphovascular invasion; sLAG-3$^+$, stromal LAG-3$^+$.

One [FMO] and isotype control), the cut-off of low/high LAG-3$^+$ cells subgroups was determined by median value (21.2%, LAG-3$^+$ cells/all cells). Representative images of cell subsets involved in this study are presented in online supplementary figure 2.

Statistical analyses

Data were presented as median and IQR. Non-parametric two-way tests were applied for continuous variables, and specific statistical tests are detailed in figure legends. The 5-year overall survival (OS) and disease-free survival (DFS) were estimated by the Kaplan-Meier method. The survival curves were constructed to compare subgroups in terms of clinical outcomes, and were detected by log-rank test. Univariate and multivariate Cox regression models were established to evaluate the impact of covariate on prognosis and the interaction between covariates. The statistical analyses were performed using IBM SPSS Statistics V.25.0 for windows (SPSS, Chicago, Illinois, USA), and two-sided p<0.05 was regarded as statistically significant.

RESULTS

Stromal LAG-3$^+$ cells enrichment indicates poor clinical outcomes in patients with MIBC

In MIBC, CD8$^+$ T cells and CD4$^+$ T cells are the main cellular source of the LAG-3 (online supplementary figure 3A). LAG-3$^+$ cells distribution was evaluated on TMA using IHC (representative stained images are illustrated in online supplementary figure 3B). Compared with intraepithelial area, LAG-3$^+$ cells infiltration was more intensive in the stroma (online supplementary figure 3C).

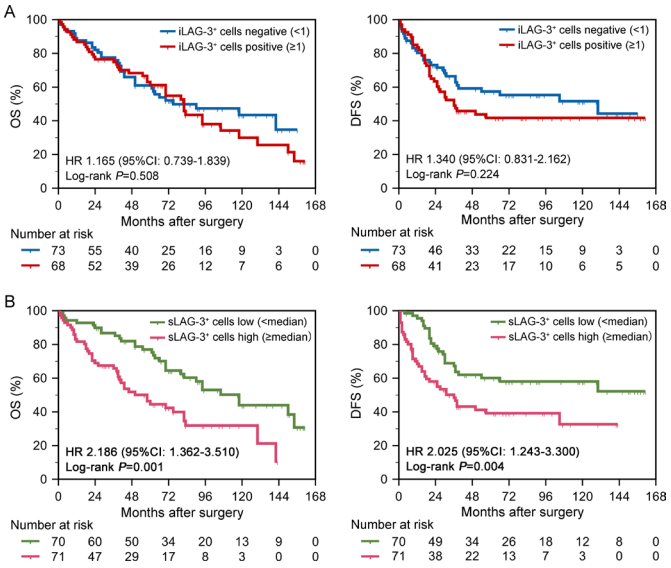

Figure 1 Association of intraepithelial LAG-3$^+$ (iLAG-3$^+$) cells and stromal LAG-3$^+$ (sLAG-3$^+$) cells with clinical outcome. (A–B) Kaplan-Meier analyses of overall survival (OS) (left) and disease-free survival (DFS) (right) of 141 patients with muscle-invasive bladder cancer (MIBC) stratified according to iLAG-3$^+$ cells infiltration (A) and to sLAG-3$^+$ cells infiltration (B). Data were analyzed by log-rank test.

The detailed association of sLAG-3$^+$ cells and iLAG-3$^+$ cells with patients' characteristics are listed in table 1 and online supplementary figure 3D, which demonstrate that sLAG-3$^+$ cells abundance was significantly correlated with

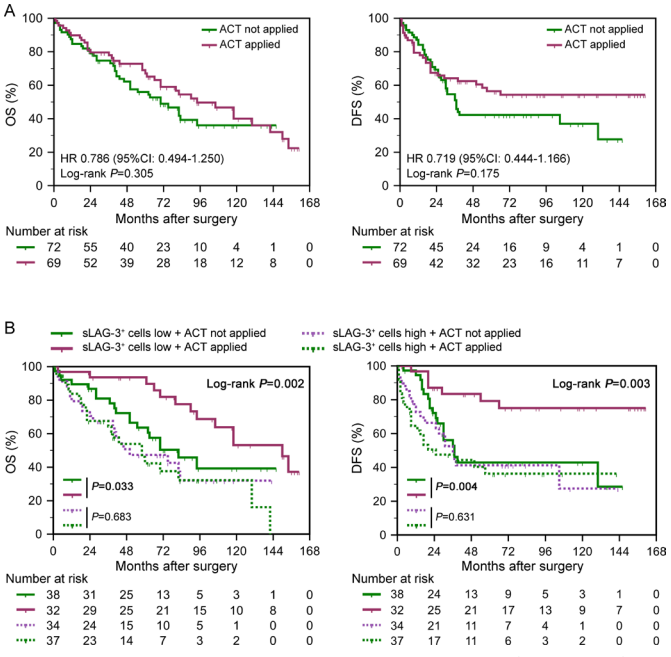

Figure 2 Relationship between stromal LAG-3$^+$ (sLAG-3$^+$) cells and adjuvant chemotherapy (ACT) responsiveness. (A–B) Kaplan-Meier analyses of overall survival (OS) (left) and disease-free survival (DFS) (right) of 141 patients with muscle-invasive bladder cancer (MIBC) stratified according to ACT application (A) and to the combination of ACT application and sLAG-3$^+$ cells infiltration (B). Data were analyzed by log-rank test.

inferior clinical features. To further elucidate the clinical significance of LAG-3$^+$ cells, we applied Kaplan-Meier analyses to compare prognosis of patients stratified by iLAG-3$^+$/sLAG-3$^+$ cells infiltration. The 5-year OS and DFS of ZSHC were 61.2% and 49.7%, respectively. Five-year OS and DFS were 61.0% and 57.4% for iLAG-3-negative tumors vs 61.2% and 41.8% for iLAG-3-positive tumors, respectively (OS: p=0.508, DFS: p=0.224; figure 1A). Notably, 5-year OS and DFS were 77.1% and 60.2% for sLAG-3-low tumors vs 44.6% and 39.2% for sLAG-3-high tumors (OS: p=0.001, DFS: p=0.004; figure 1B). Consistent with above results, univariate and multivariate Cox analyses revealed tumor-infiltrating LAG-3$^+$ cells infiltration and sLAG-3$^+$ cells infiltration were independent prognosticators for worse OS and DFS after adjustment for tumor size, stage, grade and lymphovascular invasion as confounders (online supplementary tables 3-5).

Stromal LAG-3$^+$ cells enrichment yields suboptimal ACT responsiveness in patients with MIBC

As presented in figure 2A, patients with MIBC who received adjuvant cisplatin-based chemotherapy failed to gain significant survival benefit in ZSHC (OS: p=0.305, DFS: p=0.175). To explore whether sLAG-3$^+$ cells infiltration was associated with responsiveness to ACT, we compared the prognosis of patients stratified by ACT application in different sLAG-3$^+$ cells infiltration subgroup. Intriguingly, patients treated with ACT showed a superior OS and DFS only in sLAG-3$^+$ cells-low subgroup (p=0.033, p=0.004, respectively; figure 2B). Meanwhile, analyses for the interaction between biomarkers and ACT responsiveness indicated that benefit from ACT could be predicted by sLAG-3$^+$ cells infiltration (OS: p=0.014, DFS: p=0.027) but not iLAG-3$^+$ cells infiltration (OS: p=0.886, DFS: p=0.795) or tumor-infiltrating LAG-3$^+$ cells infiltration (OS: p=0.136, DFS: p=0.115; online supplementary table 6). Collectively, these results suggested low sLAG-3$^+$ cells infiltration as an indicator for ACT application in MIBC, and implied that sLAG-3$^+$ cells enrichment potentially impeded ACT responsiveness.

Stromal LAG-3$^+$ cells enrichment identifies immunoevasive contexture in patients with MIBC

Since tumor immune microenvironment (TIME) was correlated with survival outcomes and therapeutic responsiveness,[16 17] as verified in our previous researches,[18–20] we explored the impact of sLAG-3$^+$ cells on immune contexture in MIBC. Previously, we also revealed that immune classification (immunotype A/B) based on five immune cells infiltration identified immunoevasive subtype of MIBC.[21] After evaluating the association of sLAG-3$^+$ cells infiltration with 15 immune cell types in ZSHC (figure 3A, online supplementary figure 4A), we found that patients with high sLAG-3$^+$ cells infiltration possessed a higher level of immune cells infiltration (figure 3A), and significantly presented immunotype B phenotype (figure 3B). Moreover, tumors with high sLAG-3$^+$ cells infiltration showed protumor cells abundance (regulatory T cells: p=0.002, T-helper 2: p=0.001,

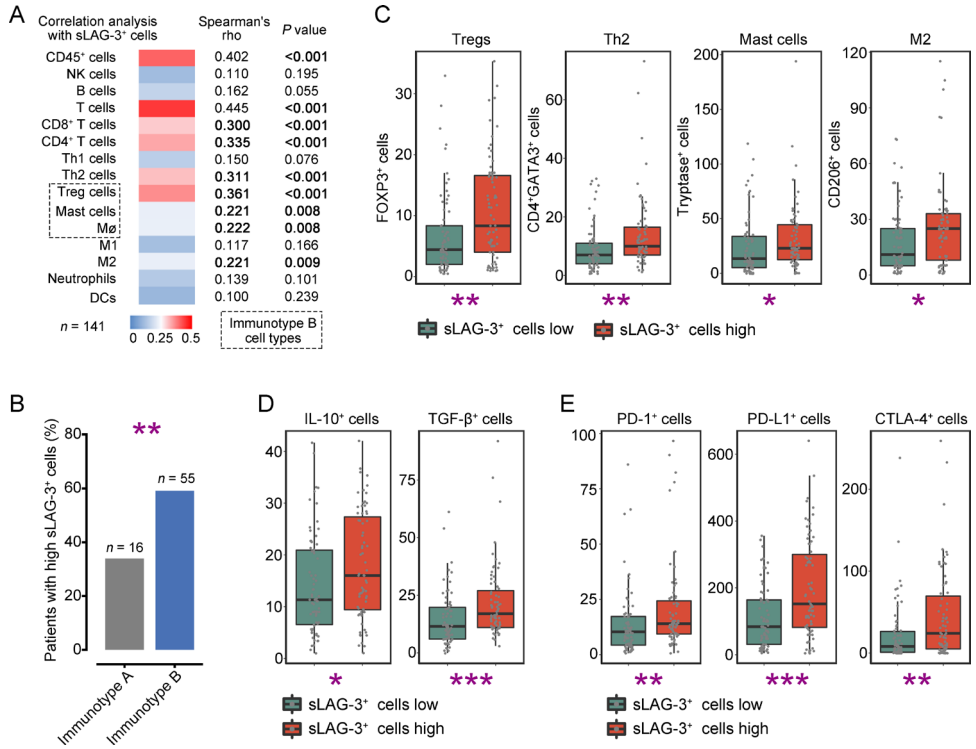

Figure 3 Identification of immunoevasive contexture based on stromal LAG-3$^+$ (sLAG-3$^+$) cells enrichment. (A) Heatmap showing Spearman's correlation analyses of immune cells with sLAG-3$^+$ cells infiltration (n=141). (B) Association of immunotype A/B with sLAG-3$^+$ cells infiltration level (n=140). Data were analyzed by χ^2 test. (C–E) Quantification analyses of immunoevasive cells (C), cytokines (D) and immune checkpoints (E) between low/high sLAG-3$^+$ cells infiltration subgroup (n=141). Data were analyzed by Mann-Whiney U test, and presented as median and IQR. *P<0.05, **p<0.01, ***p<0.001.

M2: p=0.027, mast cells: p=0.023; figure 3C),[19 22 23] which conformed with the immunoevasive microenvironment marked by immunotype B classification. Meanwhile, recent studies consider that interleukin (IL)-10 and transforming growth factor (TGF)-β as immunosuppressive cytokines are underlying mechanisms of immunoevasion.[24 25] Our results pointed that IL-10$^+$ and TGF-β$^+$ cells were highly infiltrated in sLAG-3$^+$ cells-high subgroup (p=0.020, p<0.001, respectively; figure 3D, online supplementary figure 4B). Moreover, patients with high sLAG-3$^+$ cells significantly possessed more other ICK-positive cells infiltration (PD-1: p=0.003, PD-L1: p<0.001, CTLA-4: p=0.004, TIM-3: p<0.001, TIGIT: p=0.001; figure 3E, online supplementary figure 5A-C). Together, our data indicated that sLAG-3$^+$ cells enrichment remodeled TIME characterized by overexpressed immunoevasive cells and cytokines, which might promote adverse prognosis and suboptimal ACT benefit in MIBC.

Stromal LAG-3$^+$ cells enrichment shapes CD8$^+$ T cells dysfunction in MIBC

As shown in figures 3A and 4A, patients with sLAG-3$^+$ cells enrichment contained more CD8$^+$ T cells infiltration (p=0.004), which was commonly considered as a prognosticator for better OS.[26] To reconcile why sLAG-3$^+$ cells-high subgroup possessed inferior outcomes and immunoevasive contexture despite CD8$^+$ T cells abundance, we analyzed the OS of patients stratified by CD8$^+$ T cells infiltration in different sLAG-3$^+$ cells infiltration subgroup. Interestingly, patients with low sLAG-3$^+$ cells infiltration gained survival benefit from CD8$^+$ T cells abundance (p=0.003, figure 4B). However, accumulated CD8$^+$ T cells failed to improve patients' survival in sLAG-3$^+$ cells-high subgroup (p=0.327, figure 4B), implying that sLAG-3$^+$ cells enrichment was associated with CD8$^+$ T cells dysfunction. We further conducted flow cytometry (FCM) analyses using 32 fresh resected samples to investigate the functional state of CD8$^+$ T cells in patients with MIBC. LAG-3$^+$ cells were basically CD45$^+$ immune cells (online supplementary figure 2A), which conformed to the previous studies. Results confirmed that CD8$^+$ T cells infiltrated in LAG-3$^+$ cells-high subgroup presented exhausted phenotype with decreased cytotoxicity (interferon (IFN)-γ: p=0.021, GZMB: p<0.001; figure 4C) and elevated expression of ICKs (PD-1: p=0.008, CTLA-4: p=0.001, TIM-3: p=0.007, figure 4D; LAG-3: p=0.004, TIGIT: p<0.001, online supplementary figure 6A). The multi-index markers analyses further illustrated the positive association of LAG-3 with CD8$^+$ T cells exhaustion in MIBC (online supplementary figure 6B). Consequently, these observations illustrated that sLAG-3$^+$ cells shaped CD8$^+$ T cells dysfunction, possibly through the immunoevasive contexture or LAG-3-mediated inhibitory signals.[10]

Association of LAG-3 expression with molecular subtypes in patients with MIBC

Growing studies demonstrated that molecular features of MIBC provided a promising avenue for prognostic stratification and personalized therapy.[27] Remarkably, we found that LAG-3 mRNA in TCGA-BLCA cohort was

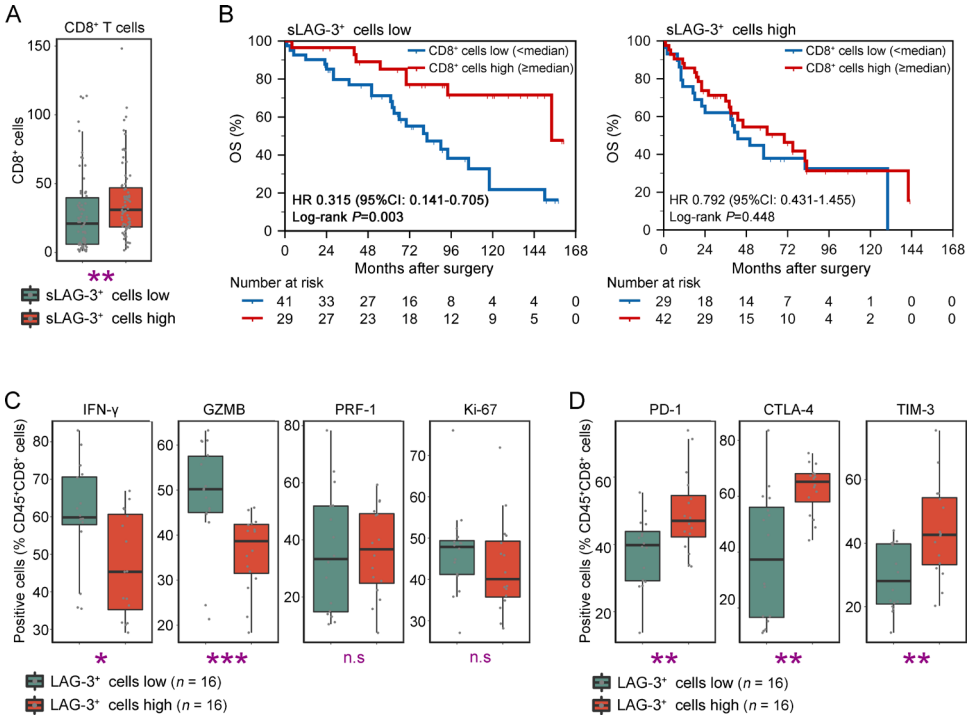

Figure 4 Characterization of CD8$^+$ T cells function based on lymphocyte activation gene 3 (LAG-3)$^+$ cells infiltration. (A) Quantification analyses of CD8$^+$ T cells between low/high stromal LAG-3$^+$ (sLAG-3$^+$) cells infiltration subgroup (n=141). Data were analyzed by Mann-Whiney U test, and presented as median and IQR. (B) Kaplan-Meier analyses of OS according to CD8$^+$ T cells infiltration in low (left, n=70) and high (right, n=71) sLAG-3$^+$ cells infiltration subgroup. Data were analyzed by log-rank test. (C–D) Flow cytometric analyses of cytotoxic/proliferative profile (C) and exhausted profile (D) of CD45$^+$CD8$^+$ T cells between low/high LAG-3$^+$ cells infiltration subgroup (n=32). Data were analyzed by Mann-Whiney U test, and presented as median and IQR. *P<0.05, **p<0.01, ***p<0.001. 'n.s.', not significant.

differentially expressed in molecular subtypes across five classification systems, and LAG-3 mRNA was highly accumulated in basal subtype of MIBC consistently (figure 5A, online supplementary figure 7). Furthermore, we defined signatures of molecular feature to validate the association between LAG-3 mRNA expression and molecular subtype. Likewise, we applied median value of LAG-3 mRNA expression to determine LAG-3-low and LAG-3-high tumors. Patients with high LAG-3 expression contained elevated basal and p53-like signature score, yet decreased luminal signature score (p<0.001, p=0.012, p<0.001, respectively; figure 5B). Considering that various molecular subtypes have distinct genomic alterations and potential therapeutic strategy,[28] we further focused on profiles of key MIBC gene mutations and therapy-associated signatures between different LAG-3 expression subgroup. As characteristics of basal subtype, abundant TP53 and RB1 gene mutations were observed in LAG-3-high tumors (p<0.001, p=0.017, respectively; figure 5C). In compatible with above findings, cell cycle pathway and proliferation signature score were higher in LAG-3-high tumors (p<0.001, p<0.001, respectively; figure 5D). Also, FGFR3 gene mutations were strongly enriched in LAG-3-low tumors, which agreed with features of luminal subtype (p<0.001, figure 5C). Additionally, LAG-3-low tumors presented high level of FGFR3 activation and FGFR3-coexpressed genes signature score (p<0.001, p<0.001, respectively; figure 5E), which might be sensitive to FGFR3-targeted therapies. The EGFR signature, ICKs and antigen-presenting signature were significantly activated in LAG-3-high tumors (EGFR signaling: p<0.001, EGFR ligands: p<0.001, ICKs: p<0.001, antigen-presenting: p<0.001; figure 5E), suggesting that EGFR-targeted drugs and immunotherapy are worth exploring in LAG-3-high patients. Cumulatively, our results reflected that LAG-3 mRNA expression was associated with luminal and basal subtypes of MIBC, and LAG-3 expression could possibly be a companion biomarker for individualized targeted therapies.

DISCUSSION

In this work, we reported that sLAG-3$^+$ cells were associated with adverse outcomes and chemotherapeutic resistance. In contrast, iLAG-3$^+$ cells infiltrated fewer in tumors and failed to be a prognosticator in MIBC. Expanding researches pointed that tumor immune-profiling and immune contexture inevitably touched the prognosis and therapeutic efficacy of patients,[16 17] which was certified previously in our studies.[18–21] Current findings revealed that LAG-3 expressed on CD8$^+$ T cells negatively regulated T cells cytotoxicity and activation, and LAG-3 expressed on CD4$^+$ T cells reshaped its phenotype to trigger an immunosuppressive function,[10] supporting our observation that sLAG-3$^+$ cells marked an immunoevasive microenvironment with CD8$^+$ T cells dysfunction.

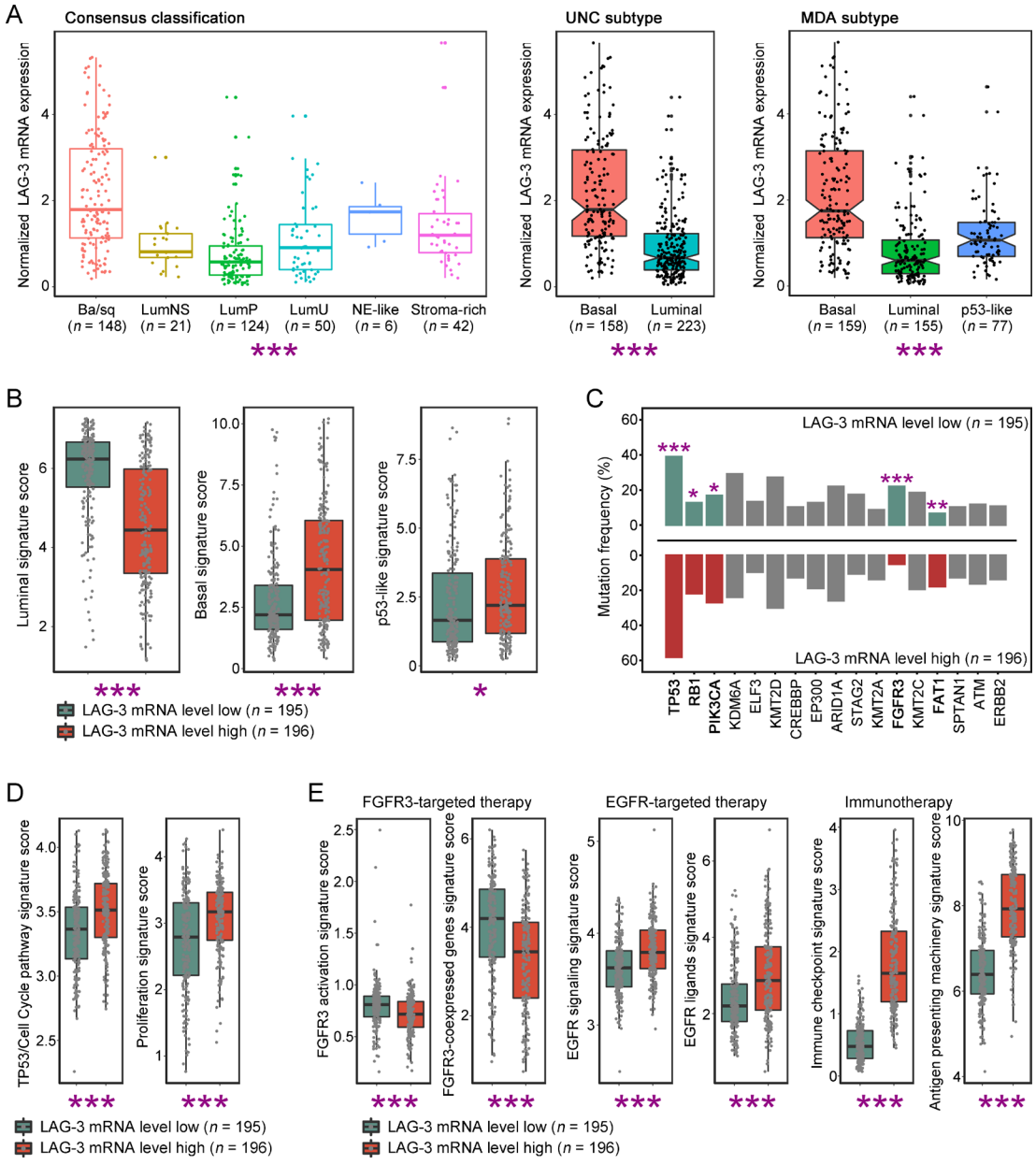

Figure 5 Features of molecular subtypes based on lymphocyte activation gene 3 (LAG-3) gene expression. (A) Quantification analyses of normalized LAG-3 mRNA expression in TCGA-BLCA database across molecular classification systems (n=391). Data were analyzed by Kruskal-Wallis H test (Consensus/MDA classification) and Mann-Whiney U test (UNC classification), and presented as median and IQR. (B) Quantification analyses of molecular subtype signatures between low/high LAG-3 mRNA expression subgroup (n=391). Data were analyzed by Mann-Whiney U test, and presented as median and IQR. (C) Association of genes mutation frequency with LAG-3 mRNA expression level (n=391). Data were analyzed by χ^2 test. (D–E) Quantification analyses of cell cycle-associated (D) and therapy-associated (E) gene signatures between low/high LAG-3 mRNA expression subgroup (n=391). Data were analyzed by Mann-Whiney U test, and presented as median and IQR. *P<0.05, **p<0.01, ***p<0.001.

Therefore, the poor survival and ACT resistance in sLAG-3$^+$ cells-high subgroup were reasonable, reflecting the interaction between cancer and immune system. Additionally, ACT in combination with LAG-3 blockade could be investigated in further researches of MIBC.

Currently, ICB therapy showed a confirmed promising efficacy in advanced bladder cancer, by restoring and boosting antitumor immune response to conquer tumor escape. However, only a small proportion of patients with MIBC obtained durable remission from ICB therapy in clinical trials (nivolumab: 19.6%, atezolizumab: 13.4%),[29] uncovering that a future emphasis on ICB therapy is to find combination-based strategies to optimize effectiveness. Given its significant role in T cells exhaustion, LAG-3 has been evaluated as a potential ICB target in malignancies and autoimmune diseases.[10] Our preclinical data based on samples of patients with MIBC demonstrated LAG-3$^+$ cells infiltration was strongly correlated

with CD8+ T cells dysfunction and ICK expression (PD-1/PD-L1/CTLA-4), supporting further evaluation of LAG-3 targeted agent for single or combined ICB therapy in clinical trials of bladder cancer.

The molecular features of MIBC were gradually unveiled and reached a consensus,[30 31] which could unmask tumor biological properties and guide therapeutic options. We discovered that basal subtype was enriched in LAG-3 mRNA-high tumors, which was characterized with EGFR signaling activation and immunotherapeutic indication. Meanwhile, the mutation of TP53 gene and TP53-related cell proliferation pathway were upregulated in LAG-3 mRNA-high tumors, which could promote tumor progression and chemotherapeutic resistance.[32] Moreover, tumors with low LAG-3 expression presented luminal subtype with potential FGFR3-targeted efficacy. The association between LAG-3 expression and molecular subtypes shaped a novel direction of individualized treatment, suggesting LAG-3 expression abundance as a companion biomarker for application of immunotherapy and EGFR-targeted approach, and yet resistance to FGFR3-targeted therapy. However, verification of above findings at the cellular level and LAG-3 blockade combined with targeted therapies warrant further investigation.

CONCLUSION

In summary, this study reported that sLAG-3+ cells abundance was an independent predictor for inferior prognosis and ACT resistance, and explicated the role of sLAG-3+ cells in immunoevasive contexture with CD8+ T cells dysfunction in MIBC. Molecular features of LAG-3-high tumors implied guiding significance of LAG-3 expression in personalized approaches to immunotherapy, EGFR-targeted therapy and FGFR3-targeted therapy. We recommended that future researches could focus on LAG-3+ cells infiltration as a biomarker in the therapeutic landscape of MIBC, and its potential as a clinical target for monotherapy and combined therapy.

Author affiliations
[1]Department of Biochemistry and Molecular Biology, School of Basic Medical Sciences, Fudan University, Shanghai, China
[2]Department of Urology, Zhongshan Hospital, Fudan University, Shanghai, China
[3]Department of Urology, Fudan University Shanghai Cancer Center, Shanghai, China
[4]Department of Urology, Shanghai Ninth People's Hospital, Shanghai Jiao TongUniversity School of Medicine, Shanghai, China
[5]Department of Urology, Ruijin Hospital, Shanghai Jiao Tong University School of Medicine, Shanghai, China

Acknowledgements The authors would like to thank Dr Lingli Chen (Department of Pathology, Zhongshan Hospital, Fudan University, Shanghai, China) and Dr Peipei Zhang (Department of Pathology, Ruijin Hospital, Shanghai Jiao Tong University School of Medicine, Shanghai, China) for their excellent pathological technology help.

Contributors HZ, QZ, ZW and HZ for acquisition of data, analysis and interpretation of data, statistical analysis and drafting of the manuscript; ZL, QH, JW, YC, QB, YX, YW, LX, BD and JG for technical and material support; LL, YZ and JX for study concept and design, analysis and interpretation of data, drafting of the manuscript, obtained funding and study supervision. All authors read and approved the final manuscript.

Funding This study was funded by grants from National Natural Science Foundation of China (31770851, 81702496, 81702497, 81702805, 81772696, 81872082, 81902556, 81902563, 81902898, 81974393), National Key R&D Program of China (2017YFC0114303), Shanghai Municipal Natural Science Foundation (16ZR1406500, 17ZR1405100, 19ZR1431800), Guide Project of Science and Technology Commission of Shanghai Municipality (17411963100), Shanghai Sailing Program (18YF1404500, 19YF1407900, 19YF1427200), Shanghai Municipal Commission of Health and Family Planning Program (20174Y0042, 201840168, 20184Y0151), Fudan University Shanghai Cancer Center for Outstanding Youth Scholars Foundation (YJYQ201802) and Shanghai Cancer Research Charity Center.

Disclaimer All the study sponsors have no roles in the study design, in the collection, analysis and interpretation of data.

Competing interests None declare.

Patient consent for publication Not required.

Ethics approval The study followed the Declaration of Helsinki and was approved by the Clinical Research Ethics Committee of Zhongshan Hospital, Fudan University Shanghai Cancer Center, Ruijin Hospital and Shanghai General Hospital. Signed informed consent was obtained from each patient.

Provenance and peer review Not commissioned; externally peer reviewed.

Data availability statement Data are available on reasonable request. All data generated that are relevant to the results presented in this article are included in this article. Other data that were not relevant for the results presented here are available from the corresponding author Dr Xu on reasonable request.

ORCID iD
Jiejie Xu http://orcid.org/0000-0001-7431-9063

REFERENCES

1 Burger M, Catto JWF, Dalbagni G, *et al*. Epidemiology and risk factors of urothelial bladder cancer. *Eur Urol* 2013;63:234–41.
2 Alfred Witjes J, Lebret T, Compérat EM, *et al*. Updated 2016 EAU guidelines on muscle-invasive and metastatic bladder cancer. *Eur Urol* 2017;71:462–75.
3 Donat SM, Shabsigh A, Savage C, *et al*. Potential impact of postoperative early complications on the timing of adjuvant chemotherapy in patients undergoing radical cystectomy: a high-volume tertiary cancer center experience. *Eur Urol* 2009;55:177–86.
4 Vlachostergios PJ, Faltas BM. Treatment resistance in urothelial carcinoma: an evolutionary perspective. *Nat Rev Clin Oncol* 2018;15:495–509.
5 Loriot Y, Necchi A, Park SH, *et al*. Erdafitinib in locally advanced or metastatic urothelial carcinoma. *N Engl J Med* 2019;381:338–48.
6 Powles T, Huddart RA, Elliott T, *et al*. Phase III, double-blind, randomized trial that compared maintenance lapatinib versus placebo after first-line chemotherapy in patients with human epidermal growth factor receptor 1/2-Positive metastatic bladder cancer. *J Clin Oncol* 2017;35:48–55.
7 Song D, Powles T, Shi L, *et al*. Bladder cancer, a unique model to understand cancer immunity and develop immunotherapy approaches. *J Pathol* 2019;249:151–65.
8 Anderson AC, Joller N, Kuchroo VK. Lag-3, Tim-3, and TIGIT: Co-inhibitory receptors with specialized functions in immune regulation. *Immunity* 2016;44:989–1004.
9 Triebel F, Jitsukawa S, Baixeras E, *et al*. LAG-3, a novel lymphocyte activation gene closely related to CD4. *J Exp Med* 1990;171:1393–405.
10 Andrews LP, Marciscano AE, Drake CG, *et al*. LAG3 (CD223) as a cancer immunotherapy target. *Immunol Rev* 2017;276:80–96.
11 Burugu S, Gao D, Leung S, *et al*. LAG-3+ tumor infiltrating lymphocytes in breast cancer: clinical correlates and association with PD-1/PD-L1+ tumors. *Ann Oncol* 2017;28:2977–84.
12 Fucikova J, Rakova J, Hensler M, *et al*. Tim-3 dictates functional orientation of the immune infiltrate in ovarian cancer. *Clin Cancer Res* 2019;25:4820–31.

13 He Y, Yu H, Rozeboom L, *et al*. LAG-3 protein expression in non-small cell lung cancer and its relationship with PD-1/PD-L1 and tumor-infiltrating lymphocytes. *J Thorac Oncol* 2017;12:814–23.
14 Fu Q, Xu L, Wang Y, *et al*. Tumor-Associated macrophage-derived interleukin-23 interlinks kidney cancer glutamine addiction with immune evasion. *Eur Urol* 2019;75:752–63.
15 Zeng H, Liu Z, Wang Z, *et al*. Intratumoral IL22-producing cells define immunoevasive subtype muscle-invasive bladder cancer with poor prognosis and superior nivolumab responses. *Int J Cancer* 2020;146:542–52.
16 Coffelt SB, de Visser KE. Immune-Mediated mechanisms influencing the efficacy of anticancer therapies. *Trends Immunol* 2015;36:198–216.
17 Fridman WH, Zitvogel L, Sautès-Fridman C, *et al*. The immune contexture in cancer prognosis and treatment. *Nat Rev Clin Oncol* 2017;14:717–34.
18 Jiang Q, Fu Q, Chang Y, *et al*. $CD19^+$ tumor-infiltrating B-cells prime $CD4^+$ T-cell immunity and predict platinum-based chemotherapy efficacy in muscle-invasive bladder cancer. *Cancer Immunol Immunother* 2019;68:45–56.
19 Liu Z, Zhu Y, Xu L, *et al*. Tumor stroma-infiltrating mast cells predict prognosis and adjuvant chemotherapeutic benefits in patients with muscle invasive bladder cancer. *Oncoimmunology* 2018;7:e1474317.
20 Zhou L, Xu L, Chen L, *et al*. Tumor-Infiltrating neutrophils predict benefit from adjuvant chemotherapy in patients with muscle invasive bladder cancer. *Oncoimmunology* 2017;6:e1293211.
21 Fu H, Zhu Y, Wang Y, *et al*. Identification and validation of stromal immunotype predict survival and benefit from adjuvant chemotherapy in patients with muscle-invasive bladder cancer. *Clin Cancer Res* 2018;24:3069–78.
22 De Monte L, Reni M, Tassi E, *et al*. Intratumor T helper type 2 cell infiltrate correlates with cancer-associated fibroblast thymic stromal lymphopoietin production and reduced survival in pancreatic cancer. *J Exp Med* 2011;208:469–78.
23 Mantovani A, Sozzani S, Locati M, *et al*. Macrophage polarization: tumor-associated macrophages as a paradigm for polarized M2 mononuclear phagocytes. *Trends Immunol* 2002;23:549–55.
24 Colak S, Ten Dijke P. Targeting TGF-β signaling in cancer. *Trends Cancer* 2017;3:56–71.
25 Lamichhane P, Karyampudi L, Shreeder B, *et al*. Il10 release upon PD-1 blockade sustains immunosuppression in ovarian cancer. *Cancer Res* 2017;77:6667–78.
26 Masson-Lecomte A, Rava M, Real FX, *et al*. Inflammatory biomarkers and bladder cancer prognosis: a systematic review. *Eur Urol* 2014;66:1078–91.
27 Knowles MA, Hurst CD. Molecular biology of bladder cancer: new insights into pathogenesis and clinical diversity. *Nat Rev Cancer* 2015;15:25–41.
28 Felsenstein KM, Theodorescu D. Precision medicine for urothelial bladder cancer: update on tumour genomics and immunotherapy. *Nat Rev Urol* 2018;15:92–111.
29 Ghatalia P, Zibelman M, Geynisman DM, *et al*. Approved checkpoint inhibitors in bladder cancer: which drug should be used when? *Ther Adv Med Oncol* 2018;10:1758835918788310.
30 Robertson AG, Kim J, Al-Ahmadie H, *et al*. Comprehensive molecular characterization of muscle-invasive bladder cancer. *Cell* 2017;171:540–56.
31 Kamoun A, de Reyniès A, Allory Y, *et al*. A consensus molecular classification of muscle-invasive bladder cancer. *Eur Urol* 2020;77:420–33.
32 Muller PAJ, Vousden KH. Mutant p53 in cancer: new functions and therapeutic opportunities. *Cancer Cell* 2014;25:304–17.